Redox Biology 16 (2018) 97–103

Contents lists available at ScienceDirect

Redox Biology

journal homepage: www.elsevier.com/locate/redox

AKT-independent activation of p38 MAP kinase promotes vascular calcification

Youfeng Yang[a,1], Yong Sun[a,1], Jianye Chen[a], Wayne E. Bradley[b], Louis J. Dell'Italia[b], Hui Wu[c], Yabing Chen[a,d,*]

[a] Department of Pathology, University of Alabama at Birmingham, 1825 University Blvd, 614 Shelby Biomedical Research Building, Birmingham, AL 35294, USA
[b] Department of Medicine, University of Alabama at Birmingham, USA
[c] Department of Pediatric Dentistry, University of Alabama at Birmingham, USA
[d] Research Department, Veterans Affairs Birmingham Medical Center, Birmingham, AL, USA

ARTICLE INFO

Keywords:
Oxidative stress
Vascular calcification
P38 MAPK
AKT
Runx2

ABSTRACT

Vascular calcification is prevalent in patients with atherosclerosis, and oxidative stress promotes pathogenesis of atherosclerosis. We have previously reported that activation of AKT by oxidative stress induces vascular calcification. Using sodium dichloroacetate (DCA), a previously reported small molecule inhibitor of AKT, the present studies uncovered an AKT-independent mechanism in regulating vascular calcification.

We found that DCA dose-dependently induced calcification of vascular smooth muscle cells (VSMC) *in vitro* and aortic rings *ex vivo*. Furthermore, DCA markedly enhanced vascular calcification in atherosclerotic ApoE knockout mice *in vivo*. DCA-induced VSMC calcification was associated with increased Runx2, but not *via* activation of AKT, a key upstream signal that upregulates Runx2 during VSMC calcification. In contrast, DCA inhibited AKT activation and induced activation of p38 MAPK in calcified atherosclerotic lesions *in vivo* and calcified VSMC *in vitro*. Using a pharmacological inhibitor and shRNA for p38 MAPK, we demonstrated that inhibition of p38 MAPK blocked DCA-induced Runx2 upregulation and VSMC calcification. Furthermore, Runx2 deletion attenuated DCA-induced VSMC calcification. Immunoprecipitation analysis revealed association of p38 MAPK with Runx2, which was enhanced by DCA treatment. Knockdown p38 MAPK inhibited DCA-induced Runx2 transactivity, supporting the function of p38 MAPK in regulating Runx2 transactivity.

Our studies have uncovered a new function of DCA in regulating vascular calcification, *via* AKT-independent activation of p38 MAPK. Furthermore, we have identified novel interaction between p38 MAPK and Runx2 enhances Runx2 transactivity, thus promoting VSMC calcification. These results revealed a novel signaling mechanism underlying DCA-induced vascular calcification, and offer opportunities to identify new therapeutic targets.

1. Introduction

Atherosclerosis leads to narrowing of the vessel and many cardiovascular complications. Vascular calcification is a manifestation of the atherosclerotic lesions, which reduces elasticity and compliance of the vessel wall [1], and is an independent risk factor for subsequent cardiovascular mortality [2,3]. Previously considered a passive calcium deposition, vascular calcification has now been determined as an active cell-regulated process resembling bone modeling [4]. We and others have demonstrated that osteogenic differentiation of vascular smooth muscle cells (VSMC) is important for the development of vascular calcification [5–7].

Increased oxidative stress plays a critical role in promoting atherosclerosis [8] and vascular calcification [5]. In the atherosclerotic lesions of the high-fat-fed ApoE deficient mice ($ApoE^{-/-}$), we have shown that increased oxidative stress is associated with increased vascular calcification [7]. Using a primary VSMC culture system, we have determined that oxidative stress induces vascular calcification through activation of AKT signaling pathways that upregulate the key osteogenic transcription factor, Runx2 [5]. Furthermore, activation of AKT in

Abbreviations: ALP, alkaline phosphatase; α-SMA, smooth muscle specific α-actin; ApoE, apolipoprotein E; ColIa1, type I collagen A1; DCA, sodium dichloroacetate; ROS, reactive oxygen species; MAPK, mitogen-activated protein kinase; OC, osteocalcin; O-GlcNAcylation, O-linked β-N-acetylglucosamine modification; Runx2, runt-related transcription factor 2; shRNA, small hairpin RNA; VSMC, vascular smooth muscle cells

* Corresponding author.
E-mail address: yabingchen@uabmc.edu (Y. Chen).
[1] These authors contribute equally to the study.

https://doi.org/10.1016/j.redox.2018.02.009
Received 28 December 2017; Received in revised form 1 February 2018; Accepted 12 February 2018
Available online 21 February 2018

diabetic mice by O-GlcNAcylation also promotes VSMC calcification [9]. Consistently, constitutively activated AKT was sufficient to promote VSMC calcification *in vitro* and vascular calcification in animals *in vivo* [10]. These studies have supported the concept that activation of AKT signaling mediates oxidative stress and hyperglycemia-induced vascular calcification.

Sodium dichloroacetate (DCA) is a small molecule that has been shown to inhibit AKT activation while increasing oxidative stress in cancer cells [11,12]. Early studies have found that DCA reduce blood glucose in diabetic dogs [13] and fasting hyperglycemia in diabetic patients [14]. It has also been recently been tested in phase I clinical trials to treat patients with advanced solid tumors [15,16]. DCA exhibits potent anti-cancer activity in cancer cells [17,18] and animal models [12,19,20], *via* inducing oxidative stress that causes apoptosis in cancer cells [21,22]. Similarly, DCA exhibited protective effects on hypoxia-induced pulmonary hypertension *via* inducing apoptosis of the pulmonary smooth muscle cells [23,24]. Most recently, DCA was found to prevent injury-induced restenosis in animal models by inducing apoptosis of smooth muscle cells [25]. Although the effects of DCA on vascular calcification have not been investigated, the regulation of DCA on the pro-calcification signals, oxidative stress, AKT and cell death, suggests that it may play a role in the development of vascular calcification.

The present study determined the effect of DCA on VSMC calcification *in vitro* and in atherosclerotic ApoE$^{-/-}$ mice *in vivo*. We found that non-toxic concentrations of DCA, did not affect VSMC viability, induced calcification of VSMC in culture and increased atherosclerotic vascular calcification in atherosclerosis in mice. Furthermore, DCA induced AKT-independent activation of p38 MAPK, which directly associated with Runx2 and induced Runx2 transactivity to promote VSMC calcification. These results offer new insights into the signaling mechanisms underlying DCA-induced vascular calcification; and provide opportunities to identify new therapeutic targets for preventing calcification.

2. Materials and methods

2.1. Experimental animals [6,7]

Eight-week-old ApoE$^{-/-}$ mice, both male and female, in C57BL/6 J genetic background were fed a high-fat, high-cholesterol diet (Harlan Teklad, TD88137) with or without DCA added in the drink water (0.75 g/L) for 5 months. A total of 9 mice were characterized in each group. The drinking water was filtered and changed twice per week. The amount of DCA used was based on previously reported in rodent models [20,24,26]. Both food and fluid intake were *ad libitum* as we described previously [6,7]. All of the protocols were approved by the Institutional Animal Care and Use Committee of the University of Alabama at Birmingham.

2.2. Tissue harvest and processing

After euthanization, the heart and vasculature were perfused with sterile PBS. The heart and the aorta were dissected under a microscope and frozen in OCT embedding medium (Tissue-Tek) for serial cryosectioning [6,7]. The initial sections were collected when the first cusp became visible in the lumen of the aorta. Serial sections of 8 μm in thickness were collected from the aortic roots. Histological analysis by Hematoxylin & Eosin (H&E) staining was performed as we previously reported [10]. Descending aorta was dissected for calcium quantification and Western blot analysis.

2.3. Oil Red O staining

After fixed with 4% paraformaldehyde, 20 μmol EDTA, and 5% sucrose for 12 h, aortic root sections were stained with Oil Red O (Sigma Aldrich) and counterstained with hematoxylin [27]. Images were captured directly using Leica light microscope and the percentage of positively stained area was quantified using ImageJ software (NIH Bethesda, MD).

2.4. Aortic calcification

Calcium deposits in aortic sections were stained using Alizarin Red (Sigma Aldrich) essentially as described previously [6,7]. Stained specimens were examined microscopically (Leica M165 FC), and the percentage of positively stained area for each aortic specimen was quantified using ImageJ software (NIH Bethesda, MD).

Aortic calcium contents in descending aortas were measured as previously described [6,7]. Descending aortas were lyophilized to constant weight and decalcified with 0.6 mmol/L HCl at 37 °C for 48 h. Calcium released from the lyophilized tissues was determined colorimetrically by Arsenazo III (3, 6-bis[(2-Arsonophenyl) Azo] − 4,5-dihydroxy-2,7-naphthalenedisulfonic acid with calcium diagnostic kit; Stanbio Laboratory). The amount of vascular calcium was normalized to the dry weight of the tissues and expressed as millimolar/gram dry weight.

2.5. Immunofluorescence staining

Frozen aortic root sections were processed and immunofluorescent staining performed as we described previously [6,7], using antibodies for mouse phospho-AKT and phospho-p38 MAPK (Cell signaling). The immunofluorescence was quantified using ImageJ software.

2.6. Aortic ring culture

Descending aortas were cut into 2–3 mm rings, which were cultured in osteogenic medium containing 1% FBS with DCA (0, 1 and 5 mM) for 2 weeks. The mediums were changed every 3 days. Then aortic rings were collected, fixed and embedded in paraffin [10]. The sections were then stained by H&E for histology and Alizarin Red for calcification.

2.7. VSMC culture

Primary VSMC were isolated from mouse aorta and cultured in growth media as we described previously [5]. All experiments were performed with VSMC isolated from at least 3 animals, and experiments were performed in duplicate or triplicate as indicated, and repeated at passages 3–5.

2.8. Cell viability/proliferation assay

VSMC were grown in a 96-well for 72 h in growth media with different concentrations of DCA from 0 to 20 mM, which have been used in cell culture as previously reported [28–30]. Cell viability was determined using the MTS Cell Proliferation Assay Kit (Promega), according to manufacturer's recommendation.

2.9. Bromodeoxyuridine proliferation assay [31]

VSMC were plated on 96-well gelatin-coated plates overnight. After serum starvation, cells were exposed to DCA from 0 to 20 mM for two days. Proliferation was determined by 5-bromo-2-deoxyuridine (BrdU) incorporation using the Millipore BrdU assay kit (Millipore), and measured with a microplate reader.

2.10. In vitro VSMC calcification

VSMC calcification was performed as we previously described in osteogenic media containing 0.25 mM L-ascorbic acid and 10 mM β-glycerophosphate and 10^{-8} nM dexamethasone (Sigma Aldrich) with or without DCA for 3 weeks with media change every 3 days [5].

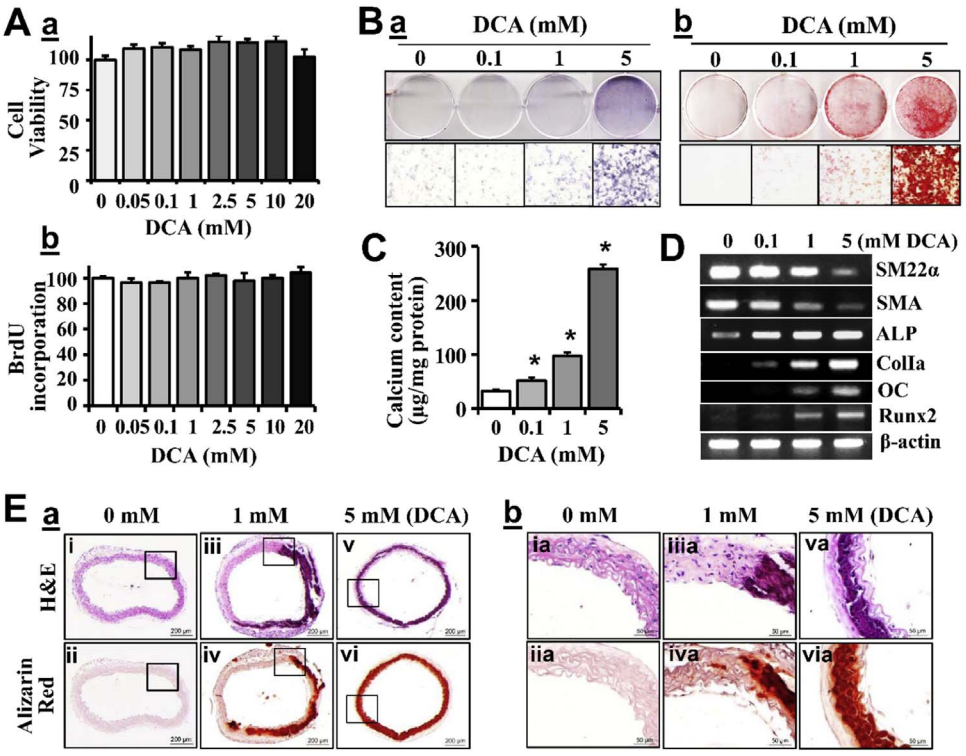

Fig. 1. DCA induces VSMC calcification. **A)** Effects of DCA on VSMC viability and proliferation, as determined by a) MTS assay and b) BrdU incorporation. Results shown are from experiments using VSMC from 3 mice, and performed in triplicate. **B&C)** Effects of DCA on VSMC calcification. VSMC were cultured in osteogenic media with DCA (0–5 mM) for up to 21 days. Calcification was determined by **a)** ALP staining at 14 days; and **b)** Alizarin Red staining at 21 days; and **C)** Quantitative measurement of calcium content at 21 days in parallel sets of experiments. Representative images of 3 independent experiments performed in duplicate are shown ($n = 3$, $^*p < 0.05$). **D)** Effects of DCA on the expression of smooth muscle and osteogenic marker genes. VSMC were exposed to DCA for 14 days, expression of smooth muscle markers SM22α, α-actin (SMA) and osteogenic markers ALP, ColIa, OC and Runx2 was determined by RT-PCR. Representative results from 3 independent experiments performed in duplicate are shown. **E)** Effects of DCA on arterial calcification *ex vivo*. Aortic rings from wild type mice were cultured in osteogenic media with DCA (0, 1 and 5 mM) for 21 days, and stained by H&E for histology (i, iii, v) and Alizarin Red (ii, iv, vi) for calcification. Higher magnification images of the boxed areas in **a** are shown in **b**. Results shown are representative images from 4 independent experiments.

Calcification was determined by Alizarin Red staining; or quantified in parallel experiments by measuring total calcium in the cell lysates by Arsenazo III method [5,6].

The effect of p38 MAPK kinase on DCA-induced VSMC calcification were determined with 10 μM SB203580 (Sigma-Aldrich).

2.11. Reverse transcriptase-polymerase chain reaction

The effect of DCA on the expression of bone-related and smooth muscle-specific gene markers was determined by RT-PCR. Total RNA was isolated from VSMC using Trizol (Invitrogen) and reverse-transcribed into cDNA. PCR was performed using specific primers for murine smooth muscle specific α-actin (SMA), SM22α, alkaline phosphatase (ALP), type I collagen A1 (Col Ia) and osteocalcin (OC), Runx2 and β-actin (loading control) as we previously described [5,6].

2.12. ALP activity assay

Cellular ALP activity was determined by ALP staining [6,32]. Briefly, VSMC were exposed to different concentrations of DCA for 2 weeks, cells were fixed with 4% PFA, and stained with an alkaline-dye mixture containing naphthol AS-BI alkaline solutions (Sigma).

2.13. Western blot analysis

Protein extracts from VSMC and mouse arteries were prepared and protein concentration was measured as we previously described [5]. Western blot analyses were performed with the use of specific antibody for p38 MAPK (Catalog# 9212), phospho-p38 MAPK (4511), ERK1/2 (9102), pERK1/2 (9101), AKT (9272), pAKT (9271) from Cell Signaling, Runx2 from MBL (D130-3) and β-actin (A5441) from Sigma Aldrich and detected with a Western blot chemiluminescence detection kit (Millipore).

2.14. Immunoprecipitation

To determine Runx2 and p38 MAPK interaction, immunoprecipitation was performed with anti-Runx2 antibody as we reported previously [9]. In brief, cell extracts were incubated with Runx2 antibody at 4 °C overnight and then mixed with protein G agarose beads (Sigma Aldrich) for 3 h. Beads were washed, and proteins pulled down were analyzed by Western blotting using specific antibodies to detect Runx2, p38 MAPK and phosphorylated p38 MAPK.

2.15. Lentiviral transduction

Lentivirus-mediated p38 MAPK knockdown or Runx2 overexpression was performed as previously described [5,6]. Lentiviral vector encoding a 21-nucleotide p38 MAPK short hairpin RNA (shRNA) was purchased from Open Biosystems and packaged into lentiviral particles. Lentiviral construct expressing wild type Runx2 was generated as we previous described [33]. Viral transductions were performed by incubating VSMC with recombinant lentiviruses in growth media supplemented with 10 μg/mL Polybrene (Sigma). After 24 h, cells were washed with PBS and kept in growth media containing puromycin for 2 weeks to select stable transfectants.

2.16. Detection of Runx2 transactivity

Runx2 transactivity was determined by a Dual-Luciferase Reporter assay with the use of p6xRunx-Luc, a luciferase reporter construct containing six Runx binding elements in the promoter region as we previously reported [5]. A plasmid encoding Renilla luciferase gene downstream of a minimal SV40 promoter was used to normalize for transfection efficiency. Twenty-four hours after transfection, cells were washed and treated with 5 mM DCA for an additional 48 h. Luciferase activities were determined with the Dual-Luciferase assay kit (Promega).

2.17. Statistical analysis

All the data in this study are expressed as means ± SD. Differences in data between two groups were compared with Student's paired 2-tailed *t*-test. For multiple group comparison, one-way analysis of

variance followed by a Student-Newman-Keuls test was performed. A p value less than 0.05 was considered statistically significant.

3. Results

3.1. DCA induces VSMC calcification

To identify a non-toxic concentration of DCA for VSMC, we tested a serial of concentrations of DCA in culture media for up to 20 mM, which has been used in cell culture as previously reported [29,30]. At all concentrations tested, DCA did not affect VSMC viability (Fig. 1Aa) or VSMC proliferation (Fig. 1Ab). Therefore, we determined the effects of DCA on VSMC calcification at concentrations between 0.1 and 5 mM.

We found that increasing concentrations of DCA markedly induced calcification of VSMC, as determined by Alkaline Phosphate (ALP) staining (Fig. 1Ba) and Alizarin Red staining (Fig. 1Bb). Measurement of total calcium content in parallel experiments further confirmed a dose-dependent effect of DCA on VSMC calcification (Fig. 1C). Consistently, DCA decreased the expression of smooth muscle marker genes, SM22α and α-SMA, while increased the expression of bone specific markers, ALP, ColIa1, OC, and Runx2 (Fig. 1D), demonstrating that DCA induces active osteogenic differentiation of VSMC.

Furthermore, we determined the effect of DCA on calcification of the arteries and VSMC in their natural milieu, using the *ex vivo* ring culture model that we and others have previously reported [10,34]. Consistent with the *in vivo* results, we found that increasing concentrations of DCA markedly enhanced vascular calcification, as demonstrated by Alizarin Red staining (Fig. 1E, ii, iv, vi). Histological analysis by H&E showed calcification in the aortic media (Fig. 1E, i, iii, v).

3.2. DCA enhances vascular calcification in atherosclerotic ApoE$^{-/-}$ mice

The effect of DCA on vascular calcification was further characterized *in vivo* in the atherosclerotic ApoE$^{-/-}$ mice. We found that DCA treatment did not affect total atherosclerotic lesions, as determined by Oil Red O staining at the aortic root (Fig. 2A). Consistent with the observations in VSMC *in vitro* and aortic rings ex *vivo*, DCA enhanced vascular calcification in mouse arteries *in vivo* (Fig. 2B, C). Alizarin Red staining of sections at the aortic root demonstrated marked increases of calcification in the DCA-treated mice (Fig. 2B). Furthermore, measurement of the total calcium contents in the descending aortas confirmed that DCA significantly enhanced calcification in the descending aortas (Fig. 2C). These results have demonstrated that DCA uniquely enhances vascular calcification in atherosclerosis *in vivo*.

3.3. DCA induces AKT-independent activation of p38 MAPK

To determine the molecular mechanisms underlying DCA-induced VSMC calcification, we first analyzed the effects of DCA on the activation of AKT, a key upstream signal that upregulates Runx2 and promotes oxidative stress-induced VSMC calcification [5,9,10]. Similar to the observations in cancer cells [11], we found that DCA abolished AKT activation in VSMC (Fig. 3A). Among other signals that have been shown to regulate VSMC calcification [5,35], we identified that DCA specifically activated the p38 MAPK but not the extracellular signal-regulated kinases (ERK) signaling pathway in VSMC (Fig. 3A).

Consistently, decreased AKT activation was determined in the aortic root sections from mice treated with DCA (Fig. 3Ba, b); whereas increased phosphorylation/activation of p38 MAPK was demonstrated in the consecutive aortic sections for the DCA-treated mice (Fig. 3Ba, c). Furthermore, Western blot analysis demonstrated inhibited AKT activation in the descending aortas from DCA-treated mice (Fig. 3C, pAKT). In sharp contrast, DCA treatment-increased p38 MAPK activation and the Runx2 level was demonstrated in the descending aortas (Fig. 3C, pp38 MAPK, Runx2). Accordingly, the results suggest that increased activation of p38 MAPK but not AKT may contribute to the DCA-enhanced vascular calcification *in vivo*.

Using a pharmacological AKT inhibitor, we confirmed that inhibition of AKT did not affect DCA-induced activation of p38 MAPK and vascular calcification (Fig. 3D), suggesting that AKT-independent activation of p38 MAPK mediates DCA-induced VSMC calcification.

3.4. Inhibition of p38 MAPK attenuates DCA-induced VSMC calcification

The role of p38 MAPK in DCA-induced VSMC calcification was initially determined using a p38 MAPK inhibitor, SB203580. We found that p38 MAPK inhibition attenuated DCA-induced VSMC calcification, as demonstrated by Alizarin Red staining and quantitative calcium measurement in parallel experiments (Fig. 4A). Concurrently, p38 MAPK inhibitor blocked DCA-induced Runx2 upregulation, suggesting that p38 MAPK activation is critical for DCA-induced VSMC calcification *via* upregulation of Runx2.

To exclude potential side effects of the pharmacological inhibitor, we generated VSMC with p38 MAPK knockdown by specific shRNA. Western blot analysis confirmed p38 MAPK knockdown in VSMC (Fig. 4B). Consistent with the results with the p38 MAPK inhibitor, p38 MAPK knockdown blocked DCA-induced VSMC calcification. DCA-induced p38 MAPK activation and Runx2 upregulation were also abolished in the p38 MAPK knockdown VSMC, supporting the role of p38 MAPK in mediating DCA-induced Runx2 upregulation and VSMC calcification. These results have demonstrated a definitive role of DCA-activated p38 MAPK in mediating DCA-induced Runx2 upregulation and VSMC calcification.

3.5. DCA-induced p38 MAPK activation promotes VSMC calcification via Runx2

To determine whether Runx2 upregulation by DCA was necessary for DCA-induced VSMC calcification, we utilized Runx2 knockout (KO) VSMC as we previously reported [6]. DCA induced calcification of the control VSMC, which was abolished in Runx2 KO VSMC as demonstrated by Alizarin Red staining (Fig. 5Aa). Quantitative measurement of total calcium content in separate sets of experiments also confirmed

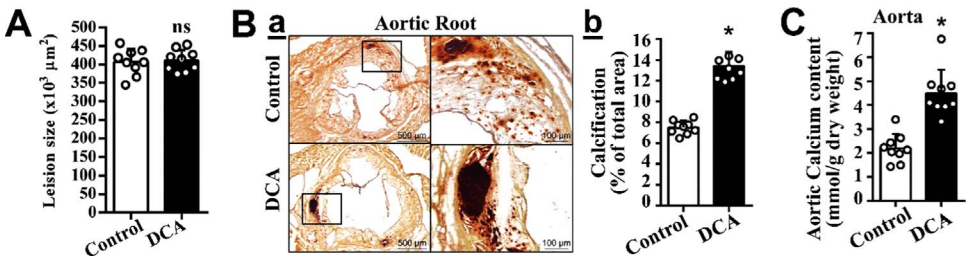

Fig. 2. DCA enhances vascular calcification in atherosclerosis mice. ApoE$^{-/-}$ mice at 8-week old were fed cholesterol diet with or without DCA in drinking water for 5 months with water change twice a week (n = 9 mice / group). **A)** Atherosclerosis lesions, determined by Oil Red O staining positive areas at the aortic root of control and DCA-treated mice using NIH ImageJ software. **B)** Vascular calcification determined in aortic roots. **a)** Representative images of aortic root sections stained with Alizarin Red are shown. Boxed areas at higher magnifications are shown to the right. **b)** Quantification of calcification in **Ba** using NIH ImageJ software. Results presented are the percentage of positively stained areas in the total area. The numbers of mice analyzed in each group are shown in each bar. Bar values are means ± SD (*$p < 0.001$). **C)** Vascular calcification determined in descending aortic tissues, by total calcium content quantification with the Arsenazo III method (*$p = 0.006$).

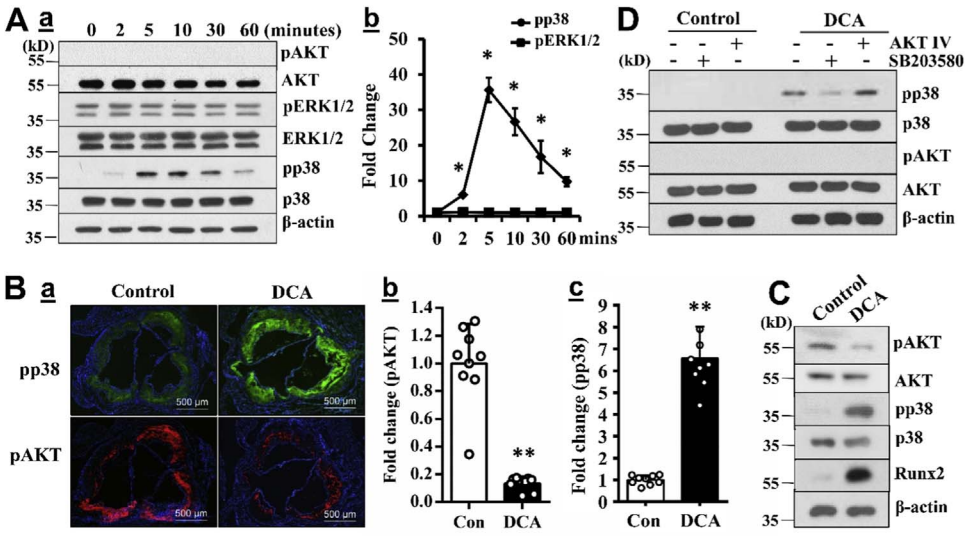

Fig. 3. DCA induces AKT-independent activation of p38 MAPK. **A)** DCA-activated cellular signaling in VSMC. Wild type VSMC were serum starved and then treated with 5 mM DCA for different durations. Phosphorylation/activation of AKT, ERK1/2 and p38 MAPK signals was determined by Western blotting analysis. a) Representative blots from 3 independent experiments are shown. The expression of β-actin was used as a loading control. b) Quantification of pp38 MAPK and pERK1/2, normalized by β-actin ($n = 3$, $^{*}p < 0.05$). **B)** and **C)** DCA-activated signals in mouse aortas. **B)** Immunofluorescent analysis of phosphorylation/activation of AKT and p38 MAPK MAPK in consecutive aortic root sections. a) Representative images (scale bar = 500 μm). b) and c) Quantification analysis of pAKT and pp38 MAPK in a). ($n = 9$, $^{**}p < 0.001$). **C)** Western blot analysis of phosphorylation/activation of AKT and p38 MAPK in descending aorta from mice with or without DCA treatment. **D)** Effects of inhibition of either AKT or p38 MAPK on DCA-induced AKT/p38 MAPK activation. VSMC were serum starved, pretreated with the inhibitors for p38 MAPK (SB203580, 10 μM) or AKT (AKT IV, 0.1 μM), and subsequently exposed to 5 mM DCA for 10 min. The activation of AKT and p38 MAPK was determined by Western blotting analysis. Representative blots from 3 independent experiments are shown.

that Runx2 KO inhibited DCA-induced VSMC calcification (Fig. 5Ab), supporting an essential role of Runx2 in DCA-induced VSMC calcification. Of note, DCA-induced p38 MAPK activation was observed in both the control cells as well as the Runx2 KO VSMC (Fig. 5Ac), indicating that Runx2 acts downstream of DCA-induced activation of p38 MAPK.

Furthermore, we determined the role of p38 MAPK in Runx2-induced VSMC calcification. Similar to our previous observation [5], overexpression of Runx2 was sufficient to induce VSMC calcification in the control VSMC, as determined by Alizarin Red staining (sh Scr, Fig. 5Ba) and quantitative calcium measurement (Fig. 5Bb). The amount of p38 MAPK and activation of p38 MAPK were not affected by Runx2 overexpression (Fig. 5Bc). In contrast, Runx2-induced VSMC calcification was inhibited in the p38 MAPK knockdown cells (sh p38, Fig. 5Ba, b), and the knockdown did not affect Runx2 expression (Fig. 5Bc). These data demonstrate that inhibition of either p38 MAPK or Runx2 was sufficient to block DCA-induced VSMC calcification, suggesting an interplay between Runx2 and p38 MAPK mediates DCA-induced VSMC calcification.

3.6. p38 MAPK interacts with Runx2 and promotes Runx2 transactivity

A direct association between p38 MAPK and Runx2 was determined by immunoprecipitation using the Runx2 antibody (Fig. 6A). In the Runx2 overexpressing VSMC, DCA treatment did not affect the protein level of Runx2 or p38 MAPK, but markedly induced p38 MAPK activation, as indicated by phosphorylation of p38 MAPK (pp38, Fig. 6Aa). Probing the Runx2-associated complex by p38 MAPK antibody revealed the association of Runx2 with p38 MAPK (Fig. 6Ab). Importantly, increased Runx2 binding to the phosphorylated p38 MAPK was identified in the DCA-treated VSMC.

The function of p38 MAPK in regulating Runx2 activity was determined by a dual luciferase reporter assay, assessing Runx2 transactivity. As shown in Fig. 6B, increased Runx2 transactivity was demonstrated in the DCA-treated VSMC (Fig. 6B, sh Scr). However, knockdown of p38 MAPK abolished DCA-induced Runx2 transactivity (Fig. 6B, sh p38), further supporting an important role of p38 MAPK in regulating DCA-induced Runx2 transactivity, which is essential for Runx2 osteogenic function.

4. Discussion

DCA has been shown to inhibit AKT activation and induce oxidative stress that lead to apoptosis of cancer cells. The potent effects of DCA on inhibiting activation of AKT, a key signaling pathway that promotes

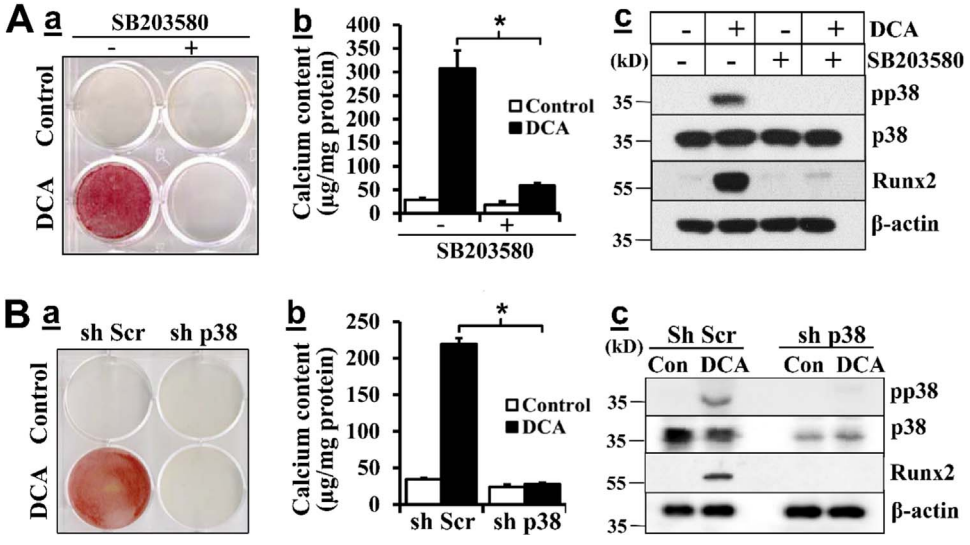

Fig. 4. Inhibition of p38 MAPK attenuates DCA-induced VSMC calcification. **A)** Effects of p38 MAPK inhibition on DCA-induced VSMC calcification. VSMC were exposed to DCA with or without p38 MAPK inhibitor SB203580 (10 μM) in osteogenic media for 21 days. **a)** Alizarin red staining for calcification. **b)** Quantification of calcium content ($n = 3$, $^{*}p < 0.01$). **c)** Western blotting analysis of Runx2 expression and p38 MAPK phosphorylation/activation. **B)** Effects of p38 MAPK knockdown on DCA-induced VSMC calcification. VSMC with control (sh Scr) or p38 MAPK specific shRNA (sh p38) were exposed to DCA in osteogenic media for 21 days. **a)** Alizarin red staining for calcification. **b)** Quantification of calcium content ($n = 3$, $^{*}p < 0.01$). **c)** Western blotting analysis of Runx2 expression and p38 MAPK phosphorylation/activation. The expression of β-actin was used as a loading control. Representative images or blots of three independent experiments are shown.

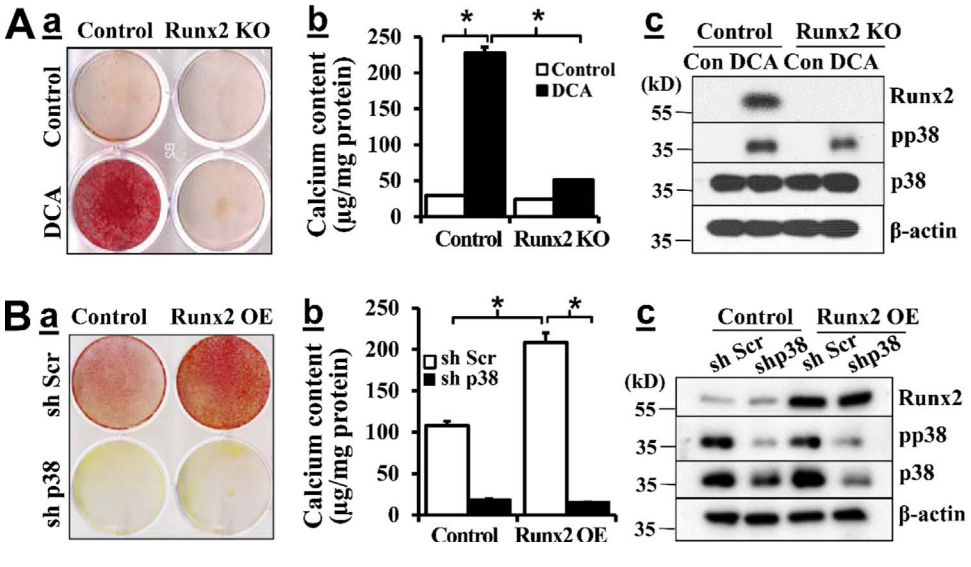

Fig. 5. DCA-induced p38 MAPK activation promotes VSMC calcification *via* Runx2. **A)** Runx2 deletion blocked DCA-induced VSMC calcification. VSMC from control and SMC-specific Runx2 deletion mice were exposed to 0 and 5 mM DCA in osteogenic media for 21 days. **a)** Alizarin red staining for calcification. Representative images of 3 experiments performed in duplicate are shown. **b)** Quantitative measurement of calcium content in separate sets of experiments (n = 3, *p < 0.001). **c)** Western blotting analysis of Runx2 expression and p38 MAPK phosphorylation/activation. **B)** Knockdown of p38 MAPK inhibited Runx2-induced VSMC calcification. Stably selected VSMC with control (sh Scr) or p38 MAPK shRNA (sh p38) were infected with lentivirus carrying control or Runx2 protein, and cultured in osteogenic media for 21 days. **a)** Alizarin red staining for calcification. Representative images of 3 independent experiments performed in duplicate are shown. **b)** Quantitative measurement of calcium content in separate sets of experiments. (n = 3, *p < 0.001). **c)** Western blotting analysis of Runx2 expression and p38 MAPK phosphorylation. Representative results of three independent experiments are shown.

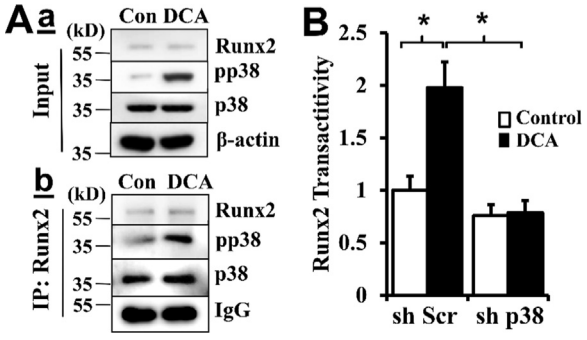

Fig. 6. p38 MAPK interacts with Runx2 and promotes Runx2 transactivity. **A)** VSMC infected with lentivirus expressing Runx2 were incubated with DCA for a short duration of 30 min. **a)** Effects of DCA on p38 MAPK activation. Western blot analysis of Runx2 expression and p38 MAPK phosphorylation. The expression of β-actin was used as a loading control. **b)** Effects of DCA on p38 MAPK and Runx2 interaction. Immunoprecipitation was performed with anti-Runx2 antibody, and binding of Runx2 to p38 MAPK and phosphorylated p38 MAPK was determined by Western blot. Representative blots of three independent experiments are shown. **B)** Knockdown of p38 MAPK inhibited DCA-induced Runx2 transactivity. Stably selected VSMC with control (sh Scr) or p38 MAPK shRNA (sh p38) were co-transfected with Runx2-expressing plasmid and the dual-luciferase reporter plasmids. The normalized luciferase activity in the control cells (sh Scr) was defined as 1 (n = 3, *$p < 0.001$).

VSMC calcification, prompted us to evaluate the function of DCA in regulating vascular calcification. Unexpectedly, we found that DCA did not inhibit but induced VSMC calcification *in vitro* and in atherosclerosis mice *in vivo*.

Although DCA was shown to be toxic to cancer cells, and cell death may promote VSMC calcification, we demonstrated that DCA-induced VSMC calcification was not due to the toxic effect of DCA on VSMC. In addition, DCA-induced vascular calcification may not be attributed to the effects of DCA on atherosclerosis in the DCA-treated mice, as we found that DCA did not affect the total atherosclerotic lesions, but induced vascular calcification in the atherosclerotic lesions in mice. By assessing the expression of the smooth muscle marker genes and osteogenic factors, we determined that DCA does-dependently induced osteogenic differentiation of VSMC, which augmented vascular calcification in atherosclerosis mice. These results add to the accumulating evidence supporting osteogenic differentiation of VSMC playing an important role in vascular calcification in atherosclerosis.

Similar to previous observations in other cells, we found that DCA also induced oxidative stress in VSMC (Supplemental Figure IA). Inhibition oxidative stress attenuated DCA-induced VSMC calcification (Supplemental Figure IB), supporting that DCA-activated oxidative stress contributes to DCA-induced VSMC calcification. As activation of AKT is required for oxidative stress-induced VSMC calcification [5] and activated AKT is sufficient to induce VSMC calcification [9,10], one would speculate that inhibition of AKT by DCA may block calcification. Unexpectedly, while activation of AKT was inhibited by DCA, vascular calcification of VSMC was still markedly increased. These data suggest that oxidative stress-activated signals, but not AKT, play a major role in DCA-induced vascular calcification. Among many signaling pathways, we identified a novel function of DCA-induced activation of p38 MAPK signaling pathway in mediating DCA-induced Runx2 upregulation and calcification of VSMC, which is independent of AKT signaling pathway. Activation of p38 MAPK is a downstream signaling pathway that has shown to be induced by oxidative stress in many cells, including cancer cells, cardiac cells and neurons [36,37]. Different from our previous observation with hydrogen peroxide-induced oxidative stress that induces AKT activation and VSMC calcification [5], DCA-induced oxidative stress was associated with AKT inhibition while activation of p38 MAPK signaling. The mechanisms underlying the differential activation of AKT and p38 MAPK signaling pathways by oxidative stress awaits further investigation. It is likely that the nature of oxidative stress, its microenvironment, and immediate targeting partners may be different, thereby inducing distinct signaling pathways, such as AKT or p38 MAPK, that lead to complex and dynamic outputs.

Our studies have revealed a unique AKT-independent interplay of p38 MAPK and Runx2 signaling axis in promoting osteogenic differentiation and calcification of VSMC. Activation of p38 MAPK signaling has been shown to promote bone cell differentiation and bone formation [38], our observation of the role of p38 MAPK activation in DCA-induced VSMC osteogenic differentiation has further supported an important function of p38 MAPK activation in promoting osteogenesis. Importantly, our studies have uncovered a previous unknown link between p38 MAPK and Runx2 in VSMC, an interaction of p38 MAPK with Runx2. Although the expression of Runx2 and p38 MAPK was not co-dependent, we found the expression of both p38 MAPK and Runx2 were indispensable for DCA-induced VSMC calcification. Our findings of increased binding of Runx2 to DCA-induced phosphorylated p38 MAPK and that p38 MAPK knockdown attenuated DCA-induced Runx2 transactivity support that DCA-induced activation of p38 MAPK contributes to increased Runx2 transactivity, thus promoting VSMC calcification. A previous study showed that MAPK is capable of phosphorylating Runx2 [39]. Therefore, it is conceivable that binding of DCA-

activated phosphorylated p38 MAPK to Runx2 may contribute to increased Runx2 transactivity and VSMC calcification. Accordingly, the DCA-induced p38 MAPK/Runx2 signaling axis may bypass the activation of AKT seen in hydrogen peroxide-induced VSMC calcification, which would explain why reduced activation of AKT by DCA did not interfere with the development of vascular calcification.

In summary, the present studies have demonstrated a previous unknown function of the small molecule DCA in promoting VSMC osteogenic differentiation and vascular calcification. Our results have also uncovered the activation of p38 MAPK signal by DCA, and interplay of p38 MAPK and Runx2 in promoting Runx2 transactivity and VSMC calcification. This new signaling mechanism underlying AKT-independent p38 MAPK activation-induced vascular calcification supports targeting p38 MAPK/Runx2 signaling axis for the prevention and treatment of vascular calcification.

Acknowledgements

We thank grant support from the National Institutes of Health (NIH), HL092215, HL136165 and DK100847, and Veterans Affairs Research Department BX000369, BX001591 (project 2) and RCS award BX003617 to YC. YY was supported by American Heart Association Grant 14POST20450117.

Disclosures

None.

Appendix A. Supplementary material

Supplementary data associated with this article can be found in the online version at http://dx.doi.org/10.1016/j.redox.2018.02.009.

References

[1] M.R. Bennett, S. Sinha, G.K. Owens, Vascular smooth muscle cells in atherosclerosis, Circ. Res. 118 (4) (2016) 692–702.
[2] P.W. Wilson, et al., Abdominal aortic calcific deposits are an important predictor of vascular morbidity and mortality, Circulation 103 (11) (2001) 1529–1534.
[3] F. Bastos Goncalves, et al., Calcification of the abdominal aorta as an independent predictor of cardiovascular events: a meta-analysis, Heart 98 (13) (2012) 988–994.
[4] A.P. Sage, Y. Tintut, L.L. Demer, Regulatory mechanisms in vascular calcification, Nat. Rev. Cardiol. 7 (9) (2010) 528–536.
[5] C.H. Byon, et al., Oxidative stress induces vascular calcification through modulation of the osteogenic transcription factor Runx2 by AKT signaling, J. Biol. Chem. 283 (22) (2008) 15319–15327.
[6] Y. Sun, et al., Smooth muscle cell-specific runx2 deficiency inhibits vascular calcification, Circ. Res 111 (5) (2012) 543–552.
[7] C.H. Byon, et al., Runx2-upregulated receptor activator of nuclear factor kappaB ligand in calcifying smooth muscle cells promotes migration and osteoclastic differentiation of macrophages, Arterioscler. Thromb. Vasc. Biol. 31 (6) (2011) 1387–1396.
[8] S. Furukawa, et al., Increased oxidative stress in obesity and its impact on metabolic syndrome, J. Clin. Invest 114 (12) (2004) 1752–1761.
[9] J.M. Heath, et al., Activation of AKT by O-linked N-acetylglucosamine induces vascular calcification in diabetes mellitus, Circ. Res. 114 (7) (2014) 1094–1102.
[10] L. Deng, et al., Inhibition of FOXO1/3 promotes vascular calcification, Arterioscler. Thromb. Vasc. Biol. 35 (1) (2015) 175–183.
[11] F. Gong, et al., Dichloroacetate induces protective autophagy in LoVo cells: involvement of cathepsin D/thioredoxin-like protein 1 and Akt-mTOR-mediated signaling, Cell Death Dis. 4 (2013) e913.
[12] E.D. Michelakis, L. Webster, J.R. Mackey, Dichloroacetate (DCA) as a potential metabolic-targeting therapy for cancer, Br. J. Cancer 99 (7) (2008) 989–994.
[13] G. Ribes, G. Valette, M.M. Loubatieres-Mariani, Metabolic effects of sodium dichloroacetate in normal and diabetic dogs, Diabetes 28 (9) (1979) 852–857.
[14] P.W. Stacpoole, G.W. Moore, D.M. Kornhauser, Metabolic effects of dichloroacetate in patients with diabetes mellitus and hyperlipoproteinemia, N. Engl. J. Med 298 (10) (1978) 526–530.
[15] Q.S. Chu, et al., A phase I open-labeled, single-arm, dose-escalation, study of dichloroacetate (DCA) in patients with advanced solid tumors, Investig. New Drugs 33 (3) (2015) 603–610.
[16] E.M. Dunbar, et al., Phase 1 trial of dichloroacetate (DCA) in adults with recurrent malignant brain tumors, Investig. New Drugs 32 (3) (2014) 452–464.
[17] Y. Duan, et al., Antitumor activity of dichloroacetate on C6 glioma cell: in vitro and in vivo evaluation, Onco Targets Ther. 6 (2013) 189–198.
[18] W.Y. Sanchez, et al., Dichloroacetate inhibits aerobic glycolysis in multiple myeloma cells and increases sensitivity to bortezomib, Br. J. Cancer 108 (8) (2013) 1624–1633.
[19] S. Bonnet, et al., A mitochondria-K+ channel axis is suppressed in cancer and its normalization promotes apoptosis and inhibits cancer growth, Cancer Cell 11 (1) (2007) 37–51.
[20] X. Zhou, et al., Dichloroacetate restores drug sensitivity in paclitaxel-resistant cells by inducing citric acid accumulation, Mol. Cancer 14 (2015) 63.
[21] A.B. Haugrud, Y. Zhuang, J.D. Coppock, W.K. Miskimins, Dichloroacetate enhances apoptotic cell death via oxidative damage and attenuates lactate production in metformin-treated breast cancer cells, Breast Cancer Res. Treat. 147 (3) (2014) 539–550.
[22] E.D. Michelakis, et al., Metabolic modulation of glioblastoma with dichloroacetate, Sci. Transl. Med. 2 (31) (2010) 31ra34.
[23] M.S. McMurtry, et al., Dichloroacetate prevents and reverses pulmonary hypertension by inducing pulmonary artery smooth muscle cell apoptosis, Circ. Res. 95 (8) (2004) 830–840.
[24] E.D. Michelakis, et al., Dichloroacetate, a metabolic modulator, prevents and reverses chronic hypoxic pulmonary hypertension in rats: role of increased expression and activity of voltage-gated potassium channels, Circulation 105 (2) (2002) 244–250.
[25] T. Deuse, et al., Dichloroacetate prevents restenosis in preclinical animal models of vessel injury, Nature 509 (7502) (2014) 641–644.
[26] I.F. Robey, N.K. Martin, Bicarbonate and dichloroacetate: evaluating pH altering therapies in a mouse model for metastatic breast cancer, BMC Cancer 11 (2011) 235.
[27] L. Gu, et al., Absence of monocyte chemoattractant protein-1 reduces atherosclerosis in low density lipoprotein receptor-deficient mice, Mol. Cell 2 (2) (1998) 275–281.
[28] C.M. Metallo, et al., Reductive glutamine metabolism by IDH1 mediates lipogenesis under hypoxia, Nature 481 (7381) (2011) 380–384.
[29] J.Y. Wong, G.S. Huggins, M. Debidda, N.C. Munshi, I. De Vivo, Dichloroacetate induces apoptosis in endometrial cancer cells, Gynecol. Oncol. 109 (3) (2008) 394–402.
[30] D. Pajuelo-Reguera, L. Alan, T. Olejar, P. Jezek, Dichloroacetate stimulates changes in the mitochondrial network morphology via partial mitophagy in human SH-SY5Y neuroblastoma cells, Int. J. Oncol. 46 (6) (2015) 2409–2418.
[31] C.H. Selzman, et al., Monocyte chemotactic protein-1 directly induces human vascular smooth muscle proliferation, Am. J. Physiol. Heart Circ. Physiol. 283 (4) (2002) H1455–H1461.
[32] R. Nakano-Kurimoto, et al., Replicative senescence of vascular smooth muscle cells enhances the calcification through initiating the osteoblastic transition, Am. J. Physiol. Heart Circ. Physiol. 297 (5) (2009) H1673–H1684.
[33] J. Chen, et al., Serum response factor regulates bone formation via IGF-1 and Runx2 signals, J. Bone Miner. Res. 27 (8) (2012) 1659–1668.
[34] R.C. Shroff, et al., Chronic mineral dysregulation promotes vascular smooth muscle cell adaptation and extracellular matrix calcification, J. Am. Soc. Nephrol. 21 (1) (2010) 103–112.
[35] Q.H. Liang, et al., Ghrelin attenuates the osteoblastic differentiation of vascular smooth muscle cells through the ERK pathway, PLoS One 7 (4) (2012) e33126.
[36] S. Kurata, Selective activation of p38 MAPK cascade and mitotic arrest caused by low level oxidative stress, J. Biol. Chem. 275 (31) (2000) 23413–23416.
[37] A. Cuenda, S. Rousseau, p38 MAP-kinases pathway regulation, function and role in human diseases, Biochim. Biophys. Acta 1773 (8) (2007) 1358–1375.
[38] M.B. Greenblatt, et al., The p38 MAPK pathway is essential for skeletogenesis and bone homeostasis in mice, J. Clin. Investig. 120 (7) (2010) 2457–2473.
[39] C.A. Simmons, J. Nikolovski, A.J. Thornton, S. Matlis, D.J. Mooney, Mechanical stimulation and mitogen-activated protein kinase signaling independently regulate osteogenic differentiation and mineralization by calcifying vascular cells, J. Biomech. 37 (10) (2004) 1531–1541.